

ORIGINAL ARTICLE

Standardization of extracellular vesicle measurements by flow cytometry through vesicle diameter approximation

E. VAN DER POL,* † ‡ A. STURK, † ‡ T. VAN LEEUWEN,* † ‡ R. NIEUWLAND † ‡ and F. COUMANS* † ‡ FOR THE ISTH-SSC-VB WORKING GROUP¹

*Department of Biomedical Engineering and Physics, Academic Medical Center, University of Amsterdam; †Department of Clinical Chemistry, Academic Medical Center, University of Amsterdam; and ‡Vesicle Observation Center, Academic Medical Center, University of Amsterdam, Amsterdam, the Netherlands

To cite this article: van der Pol E, Sturk A, van Leeuwen T, Nieuwland R, Coumans F, for the ISTH-SSC-VB Working group. Standardization of extracellular vesicle measurements by flow cytometry through vesicle diameter approximation. *J Thromb Haemost* 2018; **16**: 1236–45.

Essentials

- Platelet extracellular vesicles (EVs) concentrations measured by flow cytometers are incomparable.
- A model is applied to convert ambiguous scatter units to EV diameter in nanometer.
- Most included flow cytometers lack the sensitivity to detect EVs of 600 nm and smaller.
- The model outperforms polystyrene beads for comparability of platelet EV concentrations.

Summary. *Background:* Detection of extracellular vesicles (EVs) by flow cytometry has poor interlaboratory comparability, owing to differences in flow cytometer (FCM) sensitivity. Previous workshops distributed polystyrene beads to set a scatter-based diameter gate in order to improve the comparability of EV concentration measurements. However, polystyrene beads provide limited insights into the diameter of detected EVs. *Objectives:* To evaluate gates based on the estimated diameter of EVs instead of beads. *Methods:* A calibration bead mixture and platelet EV samples were distributed to 33 participants. Beads and a light scattering model were used to set EV diameter gates in order to measure the concentration of CD61–phycoerythrin-positive platelet EVs. *Results:* Of the 46 evaluated FCMs, 21

FCMs detected the 600–1200-nm EV diameter gate. The 1200–3000-nm EV diameter gate was detected by 31 FCMs, with a measured EV concentration interlaboratory variability of 81% as compared with 139% with the bead diameter gate. Part of the variation in both approaches is caused by precipitation in some of the provided platelet EV samples. Flow rate calibration proved essential because systems configured to 60 $\mu\text{L min}^{-1}$ differed six-fold in measured flow rates between instruments. **Conclusions**

EV diameter gates improve the interlaboratory variability as compared with previous approaches. Of the evaluated FCMs, 24% could not detect 400-nm polystyrene beads, and such instruments have limited utility for EV research. Finally, considerable differences were observed in sensitivity between optically similar instruments, indicating that maintenance and training affect the sensitivity.

Keywords: blood platelets; cell-derived microparticles; exosomes; extracellular vesicles; flow cytometry; standardization.

Correspondence: Frank Coumans, Academic Medical Center of the University of Amsterdam, Department of Biomedical Engineering & Physics (Room L0-116), Meibergdreef 9, 1105 AZ Amsterdam, the Netherlands

Tel.: +31 20 566 8977

E-mail: f.a.coumans@amc.uva.nl

¹See Appendix for a full list of Working Group Members.

Received: 28 August 2017

Manuscript handled by: P. H. Reitsma

Final decision: P. H. Reitsma, 19 February 2018

Background

Extracellular vesicles (EVs) are membrane-enclosed, cell-derived particles [1]. The pathology of many diseases, including arterial thrombosis, is characterized by elevated concentrations of circulating EVs [2]. As a basis for diagnosis, EV concentrations need to be detectable with sufficient reproducibility between laboratories. EV concentrations can be determined with flow cytometry. A flow cytometer (FCM) can simultaneously detect light scatter and fluorescence signals of single EVs at a rate in excess of 1000 s^{-1} , provided that swarming is avoided [3]. However, because of the diameter of EVs, both scatter and fluorescence signals are dim, and the smallest detectable EV diameter differs between FCMs, owing to differences in sensitivity between instruments. Because the

smallest EVs are at least an order of magnitude more frequent than the larger EVs [4,5], the minimum EV diameter detectable by each FCM will directly affect the measured EV concentration. A method for measuring EVs in the same diameter range should therefore result in comparable EV concentrations between instruments.

Two previous workshops were initiated by the Scientific Standardization Committee on Vascular Biology of the ISTH to standardize a detected diameter range of EVs [6,7]. These workshops reduced the interlaboratory variability of platelet EV concentration measurements by setting diameter gates based on measuring polystyrene beads. The second workshop accounted for differences between forward scatter (FSC) and side scatter (SSC) collection angles, by applying different beads for FSC and SSC. However, neither workshop accounted for variations in FSC and SSC collection angles, or for newer, high-sensitivity, FCM designs [8,9]. For both workshops, the diameter range of the selected EVs within the applied bead diameter gate is unknown.

Therefore, the aim of this study was to standardize concentration measurements of EVs within the same diameter range by modeling the scatter–diameter relationship for different FCMs. The scatter–diameter relationship depends on the refractive index (RI) of EVs and the FCM configuration, including fluidics, optics, electronics, and settings. In previous studies, the RI of EVs was typically assumed to be constant, with a value near 1.40 [10,11]. All RIs given in the text are for a wavelength of 488 nm. The scatter–diameter relationship can be computed for FCM configurations by the use of MATLAB scripts from Mätzler [12], based on Mie theory [13]. In

our approach, polystyrene beads are used to establish the scatter–diameter relationship for EVs [3]. Figure 1 shows the scatter–diameter relationships for three FCMs that differ in optical configuration, and therefore have different scatter–diameter relationships. Figure 1A shows FSCs and Fig. 1B and Fig. 1C show two different SSC configurations of three different FCMs. The scatter signal of a 400-nm polystyrene bead (RI = 1.61, black ball in the inset) corresponds to an EV diameter of 700 nm (Fig. 1A), 1790 nm (Fig. 1B), and 1450 nm (Fig. 1C; the orange line and the inset green ball both indicate the EV diameter for RI = 1.40) [3]. From this example, it is clear that adjustment for the differences in collection optics between instruments is essential to set comparable EV diameter gates. In the approach tested here, the scatter–diameter relationship for EVs is used to find the EV diameter gates.

The choice of EV diameter gate needs consideration. Because some FCMs are insensitive by design, an all-inclusive strategy will suffer from the least sensitive FCM, and thus ends up gating only large EVs. On the other hand, requiring all EV researchers to work only on FCMs with ‘state-of-the-art’ sensitivity is not feasible. Therefore, we decided to determine the concentrations of EVs in three different diameter gates, whereby EVs within the largest diameter gate are expected to be detectable by most FCMs, and those within the smallest diameter gate by only a few FCMs. These three ranges are 300–600 nm, 600–1200 nm, and 1200–3000 nm. Because the 1200–3000-nm diameter range of EVs considerably overlaps with platelet diameters, it is impossible to distinguish platelet-derived EVs from platelets within this diameter range.

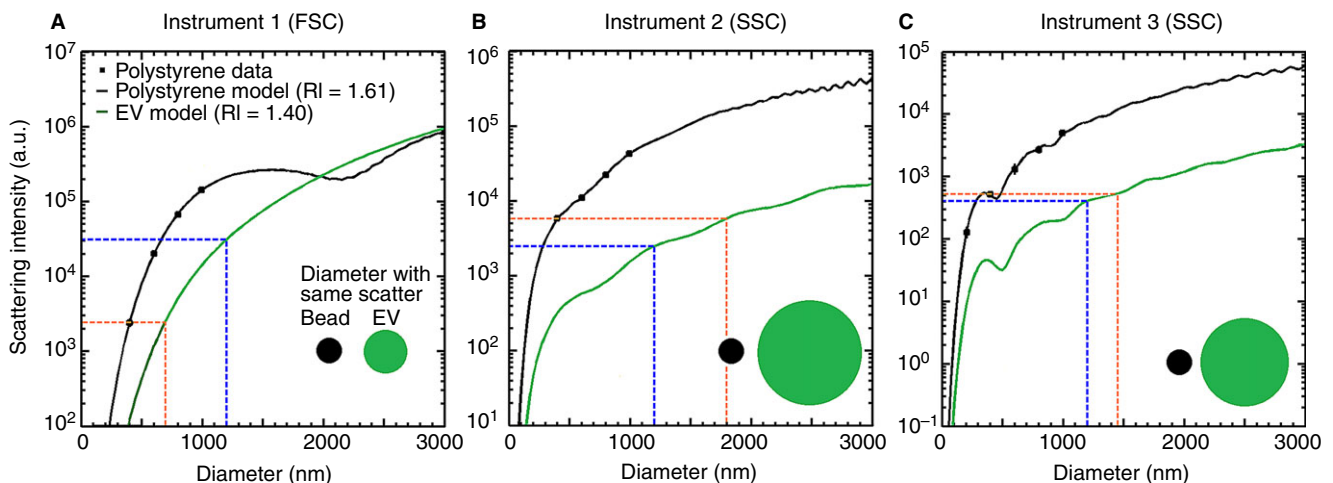


Fig. 1. Scatter–diameter relationships for three commercial flow cytometers (FCMs). The measured scatter signal for polystyrene beads (black markers) is fitted with a Mie model (black line). The scatter–diameter relationship for extracellular vesicles (EVs) is extrapolated (green line). The orange dashed line shows the scatter signal from a 400-nm polystyrene bead on the vertical axis, and the corresponding vesicle diameter on the horizontal axis. The two spheres in the inset show the relative diameter difference between the 400-nm polystyrene sphere and the vesicle with the same scatter signal. (A) BC Gallios 700 nm. (B) BD LSR II 1800 nm. (C) BC Astrios MoFlo 1430 nm. The dashed blue line shows the scatter signals corresponding to a 1200-nm vesicle for the three FCMs. a.u., arbitrary units; FSC, forward scatter; RI, refractive index; SSC, side scatter.

Objective

To evaluate a scatter–diameter model to standardize EV concentration measurements on FCMs.

Methods

Outline

Study participants first calibrated their instruments to determine the EV diameter gates that they could measure. Participants who could measure at least one EV diameter gate proceeded to measure the flow rate and CD61–phycoerythrin (PE)-stained EV samples. The EV concentration was determined on the basis of immunofluorescence and the detectable EV diameter gates. For comparison, the EV concentration was also determined for a bead diameter gate and by fluorescence alone (i.e. no diameter gate).

Participants

All participants had a publication track record on detection of EVs by flow cytometry. In addition, two participants without an EV track record but who were very knowledgeable about FCMs or standardization were invited to take part.

Samples and distribution

We distributed frozen aliquots of platelet EVs, also known as ‘platelet microparticles’. See Data S1 for additional details.

The concentrations of staining reagents were $5.2 \mu\text{g mL}^{-1}$ for lactadherin–fluorescein isothiocyanate (FITC) (Haematologic Technologies, Essex Junction, VT, USA), $0.65 \mu\text{g mL}^{-1}$ for CD61–PE (VIPL2; BD Biosciences, San Jose, CA, USA), and $1.8 \mu\text{g mL}^{-1}$ for IgG₁–PE (mouse BALB/c IgG₁, κ ; BD Biosciences). Simultaneously, an aliquot of the sample was thawed on melting ice for 1 h and diluted 1 : 7 (v/v) with phosphate-buffered saline (PBS). The sample was visually inspected for clumps. For staining, 5 μL of lactadherin–FITC and 5 μL of antibody conjugate (either CD61–PE or IgG–PE) was added to 40 μL of sample and incubated for 15 min in the dark. Then, the mixture was diluted with 550 μL of PBS. Besides isotype controls, PBS with and without staining reagent was measured.

Software and beads for standardization

The Rosetta Calibration system (Exometry, Amsterdam, the Netherlands) was used to determine the diameter gates for each flow cytometer. Rosetta Calibration consists of software and a mixture of seven types of polystyrene bead with traceable mean diameters between 100 nm and 1000 nm. Fluorescent polystyrene beads of 400 nm are

included as a marker. The bead mixture is analyzed on the FCM, with the settings for EV analysis. The measurement data are analyzed by a standalone software package that automatically recognizes the bead populations and fits a Mie model to derive the parameters describing the optical configuration of the used FCM. Starting from the manufacturer’s specification for each FCM, these optical parameters are fitted to different values for each FCM, accounting for differences in both design and FCM alignment; see [14,15] for more details. With the assumption of an RI of 1.40 for EVs [10], the scatter–diameter relationship for EVs is estimated. The output of the software is the Mie model for spheres of various RIs, including EVs (RI = 1.40) [10,15], polystyrene (RI = 1.61), and silica (RI = 1.44). Furthermore, EV diameter gates are given in scatter units that correspond to three EV diameter ranges: 1200–3000 nm, 600–1200 nm, and 300–600 nm. These gates in scatter units can then be applied in the analysis software of the user. The gates were carefully selected to avoid inflection points of the scatter–diameter relationship at gate boundaries for the included FCMs.

First assessment of sensitivity

Each participant measured the Rosetta Calibration bead mixture, and sent the data files to the coordinating laboratory. The files were analyzed with the Rosetta Calibration software to determine the detectable gates. Whenever the sensitivity was less than expected based on the FCM specifications, participants were asked to change their measurement settings to evaluate whether the sensitivity could be improved. Participants who could measure the 1200–3000-nm gate continued to perform measurements on the platelet EVs. To validate the fitted model, participants measured a silica bead mixture containing 391-nm and 772-nm silica beads (Exometry).

Flow rate calibration

Determination of the EV concentration, defined as the number of EVs per milliliter, requires the number of EVs detected and the sample volume. The measured sample volume can be derived from the product of flow rate and measurement time. Although several FCM interfaces allow setting of the flow rate in $\mu\text{L min}^{-1}$, this flow rate is typically unmonitored and requires calibration before the actual flow rate is known. We evaluated two independent methods for determining the flow rate: TruCount beads (BD Biosciences) and mass discharge. TruCount was performed as described in the product insert. Briefly, a pellet containing a known number of beads is dissolved in a known volume, and the number of beads measured per unit time is directly correlated with the sample volume processed during that time. The mass discharge is determined by weighing a sample tube before and after a 10-min measurement.

Sample measurement

Participants configured their FCMs according to local procedures. We suggested applying a flow rate of $60 \mu\text{L min}^{-1}$, measuring for 1 min, setting the scatter voltages such that no saturation occurs, and setting the fluorescent voltages such that isotype control signals are in the first log-decade. Participants who preferred a lower flow rate were asked to measure for longer time to detect a sufficient number of EVs. Participants measured the data and performed their own data analysis, and submitted the determined ungated and EV diameter-gated concentrations together with the data files to the coordinating laboratory.

Determination of reproducibility

First, we determined the EV concentration on the basis of immunofluorescence alone to establish the performance of a no diameter gate. Second, we selected polystyrene bead diameter gates for comparison with earlier bead-based approaches [4,5]. Similarly to the latest FCM workshop [7], we selected two bead diameter gates to compensate for differences between SSC and FSC. This resulted in a 400–800-nm bead diameter gate for SSC and a 600–1000-nm bead diameter gate for FSC, both which are comparable to a 1200–3000-nm EV diameter gate (FACSCanto versus Gallios). Third, the EV concentration in the 1200–3000-nm EV diameter gate was compared with those in the no diameter gate and the bead diameter gate. Furthermore, we determined EV concentrations in EV diameter gates of 600–1200 nm and 300–600 nm. Figure 2 shows the no diameter gate, bead diameter gate, 1200–3000 nm EV diameter gate, 600–1200 nm EV diameter gate and 300–600 nm EV diameter gate in a randomly selected sample. To summarize the results, for each gate we determined the coefficient of variation (CV) (ratio of standard deviation over mean) of EV concentrations from all participating FCMs. The bead diameter gates were applied centrally with FLOWJO vx (FlowJo, Ashland, OR, USA) because the scatter signals for the beads were not shown in the Exometry software. All other gating was performed by the participants. All statistical data analysis was performed in MATLAB 2014a (Mathworks, Natick, MA, USA). Data files are available upon request.

Results

Inclusion

The 33 participants registered a total of 64 FCMs. A total of 23 FCMs recorded data from platelet EV samples. Figure 3 summarizes the reasons for exclusion. Of the 64 FCMs, 18 did not return data, 15 because the participant had registered multiple (up to six) FCMs, but only intended to measure on one or two FCMs. Two FCMs

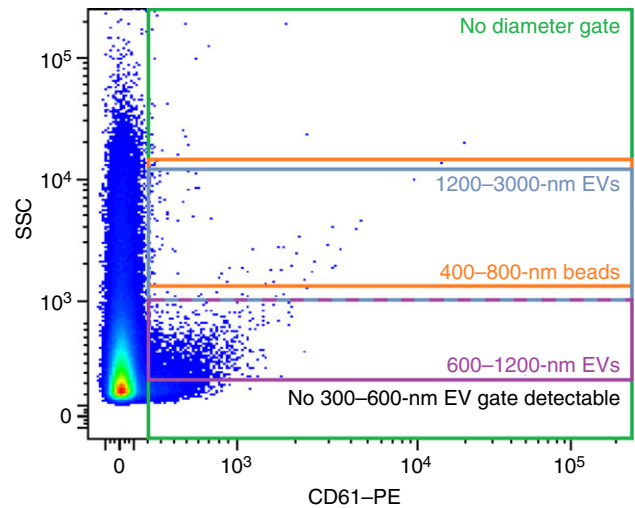


Fig. 2. Example of the five gates set on a BD FACSCanto flow cytometer. A no diameter gate (green) selects all extracellular vesicles (EVs) with CD61–phycoerythrin (PE). The 400–800-nm polystyrene bead diameter gate (orange) and the 1200–3000-nm EV diameter gate (red) overlap. The 600–1200-nm EV diameter gate (beige) is detectable, but the 300–600-nm EV diameter gate is not. SSC, side scatter.

could not be tested, owing to customs issues, and one FCM was no longer available. The remaining 46 FCMs measured the Rosetta Calibration beads to assess the sensitivity. Of these 46 FCMs, 23 were excluded, 11 because the FCMs could not measure scatter from a 400-nm fluorescent polystyrene bead, which is required for the FCM calibration, three because the laboratory had already submitted data from a similar FCM, three because they were no longer available, and three because participants did not submit any data.

FCM light scatter sensitivity

All participants measured the Rosetta Calibration beads with the FCM settings that they previously applied to study EVs (Fig. 4). Fourteen FCMs were not sensitive enough to detect 400-nm fluorescent polystyrene beads. Because detection of these 400-nm beads is essential for identification of the different bead populations, the procedure could not determine the optical configuration of the FCM, so no scatter–diameter relationship for these FCMs could be determined. In contrast to the previous workshops [6,7], we require the signals of marker beads to exceed the background noise to allow the algorithm to automatically find the peaks. Thus, a scatter signal that is dominated by noise is not adequate for reliable EV diameter determination. The model was applied to FSC for the BC EPICS XL, Gallios, Navios and Astrios and BD Influx systems [7]. Of the BC FCMs, the Astrios FCM, two of four Gallios FCMs and one of six Navios FCMs could detect the 400-nm beads. The model was applied to SSC for the remaining 30 FCMs. Among these, all five

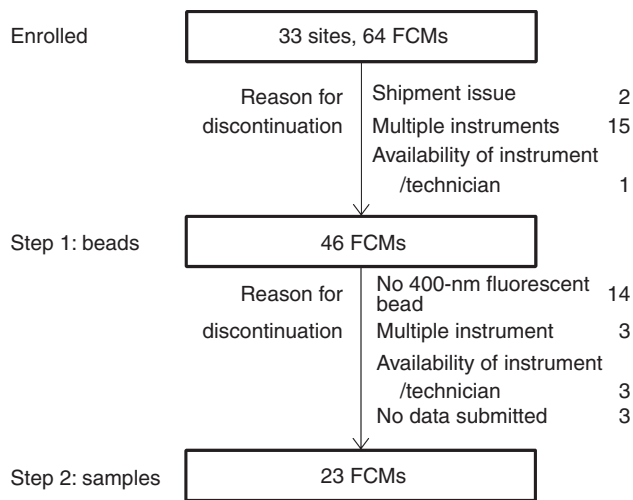


Fig. 3. Enrollment and reasons for exclusion from final result. FCM, flow cytometer.

BD Accuri C6 FCMs and one FACS Canto II FCM could not detect the 400-nm beads. For the FCMs in this study, the scatter from 400-nm polystyrene beads corresponds to vesicle diameters of 700–900 nm on FSC and 1200–1900 nm on SSC, with the exact value depending on the configuration of the FCM (Fig. 1). Thus, it is possible for FSC-sensitive FCMs to detect the 1200–3000-nm EV diameter gate, but impossible for them to detect the 600–1200-nm EV diameter gate. An FCM that cannot detect in the 600–1200-nm EV diameter gate has limited utility for EV research.

For the 32 FCMs that could detect the 400-nm fluorescent beads, the model could be applied to determine the EV diameter gates. All participants could apply the EV diameter gates in their own analysis software. The mean diameters of silica validation beads (391 nm and 772 nm) were estimated to be 373 nm (CV of 5.8%) and 772 nm (CV of 3.7%) (see Table S1 and Fig. S1 for data per FCM). The largest error translates into an uncertainty of + 100 nm/– 80 nm on the 1200-nm EV boundary. This is a small range as compared with the 700–1800-nm EV diameter corresponding to the signal of a 400-nm polystyrene bead, depending on the FCM configuration. Furthermore, the three FCMs with the largest errors in silica bead diameter estimates had relatively high CVs for bead measurements, suggesting that performance may be improved by optical alignment and/or fluidics maintenance.

Of the FCMs that could be calibrated, 32 had sufficient sensitivity to detect EVs in the 1200–3000-nm gate. Of these 32 FCMs, 22 could measure EVs in the 600–1200-nm gate, and six could measure EVs in the 300–600-nm gate.

Flow rate calibration

The sample flow rate was set to 60 $\mu\text{L min}^{-1}$ by 18 of 23 participants, and five participants used a flow rate

between 5 $\mu\text{L min}^{-1}$ and 30 $\mu\text{L min}^{-1}$ because their FCMs had better CVs at lower flow rates. Figure 5A shows the configured rate versus the rate measured with TruCount beads. The FCMs that were configured to 60 $\mu\text{L min}^{-1}$ had flow rates that varied between 20 $\mu\text{L min}^{-1}$ and 121 $\mu\text{L min}^{-1}$, which underlines the need to determine the actual flow rate when reporting a measured concentration.

The comparison between TruCount beads and mass discharge shows that these methods are in agreement with each other ($R^2 = 0.81$), and flow rates measured by mass discharge were, on average, 14% higher than flow rates measured with TruCount beads (Fig. 5B). Three participants reported sheath fluid falling into the test tube before or after the measurement time, which will result in an underestimation of the flow rate measured by mass discharge. In fact, only one mass discharge rate was below the TruCount rate. Mass discharge could not be determined for the Apogee A50, because this FCM has an actuated syringe to control the flow rate. An actuated syringe should provide a more reliable flow rate than could be determined with either TruCount or mass discharge. Because no participant made remarks about the TruCount method, the platelet EV concentrations in this article are based on flow rates determined with TruCount beads.

CV of EV concentrations

Five participants reported visible precipitation in the platelet EV samples after thawing, and the precipitation was also observed after thawing of a second aliquot. Precipitation may change the concentration and diameter distribution of CD61⁺ platelet EVs. The number of CD61⁺ platelet EVs μL^{-1} was determined within the five gates as described in Methods (Fig. 2). The ranges of CD61⁺ platelet EVs μL^{-1} were 8–85 159 (CV of 144%, 10 000-fold difference) for fluorescence only, 1–751 (CV of 139%) for the bead diameter gate, 32–875 (CV of 81%) for the 1200–3000-nm EVs, 1–16 331 (CV of 82%) for the 600–1200-nm EVs, and 2–156 906 (CV of 115%) for the 300–600-nm EVs (Figs 6 and 7). Because of the reporting of clumps, we expect that the observed variation is mostly attributable to intersample variation, and is thus not caused by the FCM and data analysis. As a contingency, the workshop also distributed erythrocyte EV samples (Data S2). For these samples, the CV was 100% for the CD235a–PE gate, 93% for the bead diameter gate, and 55% for the 1200–3000-nm EV diameter gate.

Discussion and conclusions

We applied a scatter–diameter model to reduce the inter-laboratory variability of platelet EV measurements performed in laboratories worldwide and on the most common types of FCM. Despite problems with

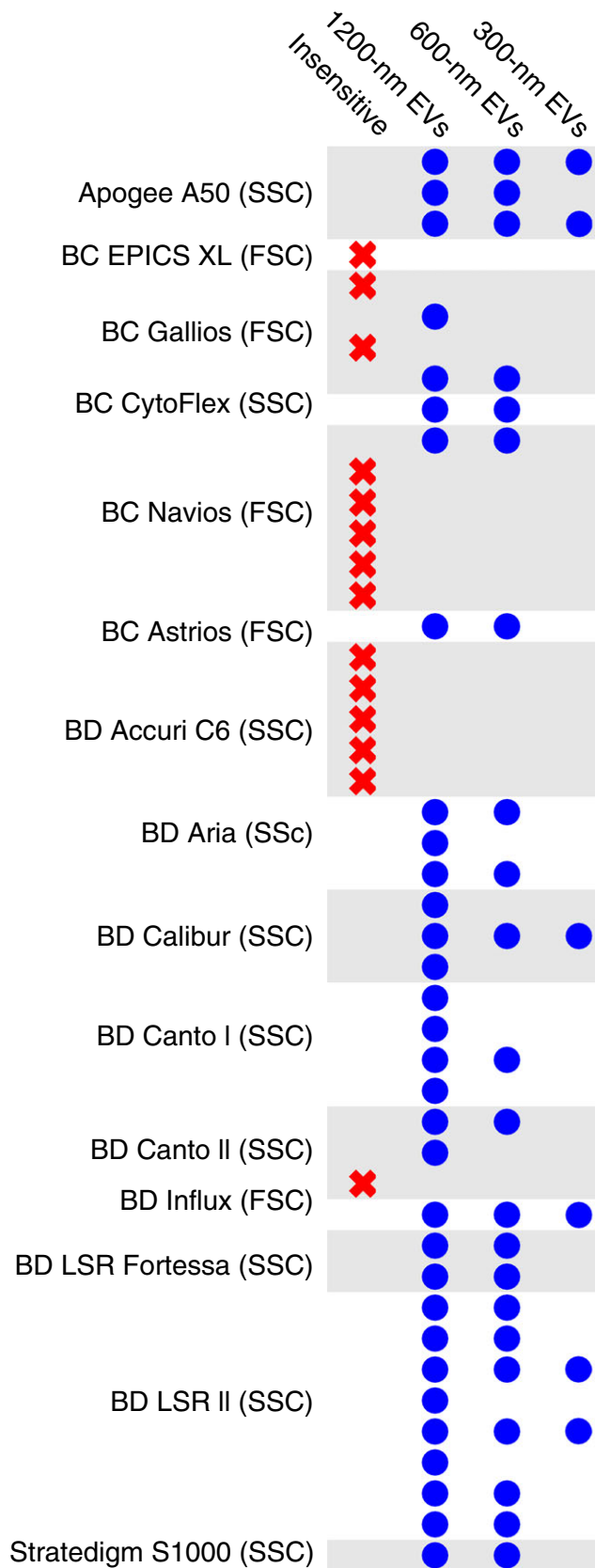


Fig. 4. Assessment of flow cytometer (FCM) sensitivity. Blue markers indicate whether an FCM was capable of detecting the signal of 1200-nm, 600-nm and/or 300-nm vesicles above the threshold level. For a number of FCMs this threshold could not be determined, because their scatter was too insensitive to detect 400-nm fluorescent polystyrene beads (red cross). Whether the model was applied to forward scatter (FSC) or side scatter (SSC) is shown in parentheses after the FCM name. EV, extracellular vesicle. [Color figure can be viewed at wileyonlinelibrary.com]

precipitation in the EV samples, we found that the CV improved from 139% to 81% for a polystyrene bead-based gate to an EV diameter-based gate, respectively. This improvement suggests that the light scattering model assuming an RI of 1.40 for EVs is a step in the right direction, which is supported by the CVs of 93% for the bead diameter gate and 55% for the 1200–3000-nm EV diameter gate for erythrocyte EV samples (Data S2). Furthermore, a scatter–diameter model converts arbitrary scatter units to nanometers, and thus provides valuable information on the measured particles. For example, an SSC gate on 400–800-nm polystyrene beads approximately detects platelet EVs of 1200–3000 nm. Thus, from the measurement data, it is not possible to tell whether CD61⁺ particles within the 1200–3000-nm gate are small platelets [16] or platelet-derived EVs. In general, if the diameter distributions of EVs and the cell of origin overlap, an EV identification marker is needed, which is so far unavailable.

For standardization, in addition to the determination of the detected diameter in nanometers, it is important to calibrate the fluorescence channels and the sample flow rate. Fluorescence channels can be calibrated to mean equivalent soluble fluorochromes [17], and the fluorescence resolution limit can be determined [18]. This is currently being evaluated for EV samples by a joint working group from the ISTH, the International Society for the Advancement of Cytometry, and the International Society for Extracellular Vesicles (evflowcytometry.org). This fluorescence information is essential to assess whether differences in EV concentrations may be attributable to differences in the fluorescence resolution limit between FCMs. Furthermore, for concentration measurements, calibration of the flow rate is essential. Both the Tru-Count beads method and the mass displacement method are adequate approaches for flow rate calibration. Tru-Count beads are applicable for all FCMs, and are easier to use.

Because EVs are commonly defined as membrane-enclosed particles with a diameter between 50 nm and 1000 nm, any FCM applied for EV research should at least be able to measure EVs within the 600–1200-nm EV diameter gate. However, to our surprise, only 22 of the 46 participating FCMs were able to measure the entire 600–1200-nm EV diameter gate (Fig. 4). This relative insensitivity can be attributed to the design, the state of

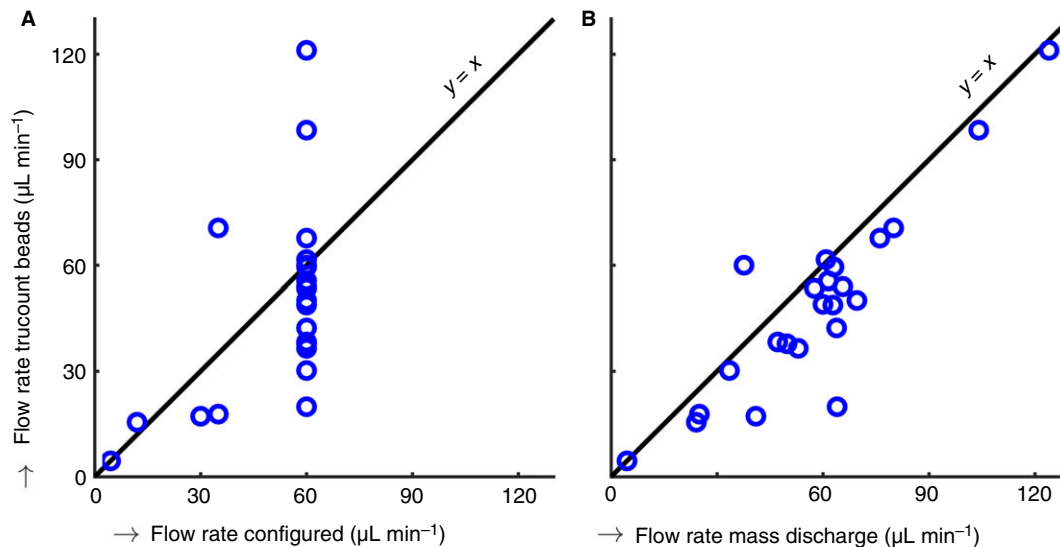


Fig. 5. Measured and configured flow rates on 23 flow cytometers. Participants typically configured the flow rate to $60 \mu\text{L min}^{-1}$ and determined the flow rate both with TruCount beads and by weight aspirated during 10 min of measurement. (A) For a configured flow rate of $60 \mu\text{L min}^{-1}$, flow rates determined by TruCount were between $20 \mu\text{L min}^{-1}$ and $121 \mu\text{L min}^{-1}$. (B) The mass discharge flow rate is 14% higher on average than the TruCount flow rate. [Color figure can be viewed at wileyonlinelibrary.com]

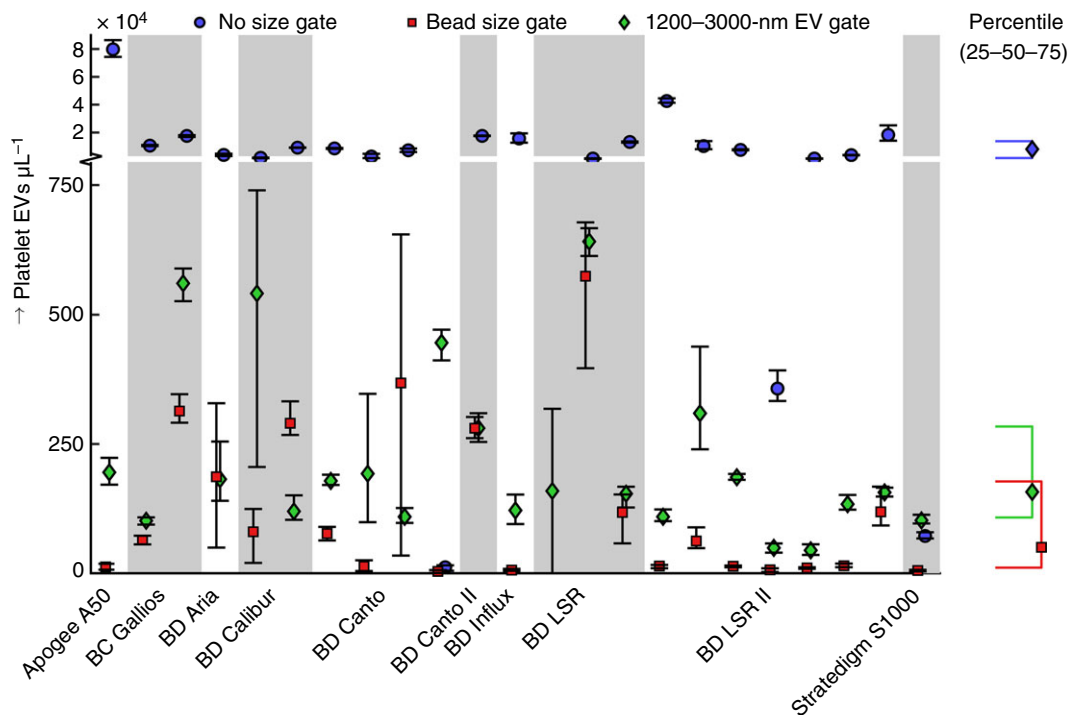


Fig. 6. Determined concentrations of platelet extracellular vesicles (EVs) on different flow cytometers (FCMs) for three different methods. In the fluorescence only gate method, events that have a CD61-phycoerythrin (PE) signal above the isotype control (CD61-PE^+) are included. In the bead diameter gate method, all CD61-PE^+ events are included if their scatter signal is within that of 400–800-nm polystyrene beads for side scatter FCMs and within that of 600–1000-nm polystyrene beads for forward scatter FCMs. In the 1200–3000-nm EV diameter gate method, CD61-PE^+ events are included if their scatter signal is in within the signal of 1200–3000-nm EVs. The markers show the minimum, maximum and median of three measurements. On the right, the 25th, 50th and 75th percentiles for all methods are shown. [Color figure can be viewed at wileyonlinelibrary.com]

maintenance and the day-to-day operational configuration of the FCM, and/or the training level of the operator. The operator training level needs to be higher for more

complex instruments such as the BD Influx or the BC Astrios. For example, the performance of the BD Accuri is most likely attributable to the FCM design. In addition,

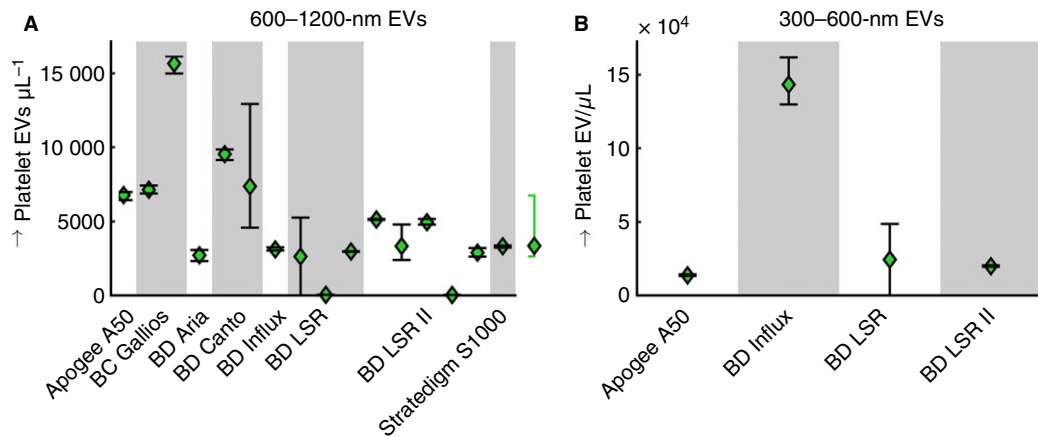


Fig. 7. Determined concentrations of platelet extracellular vesicles (EVs) on different flow cytometers for 600–1200-nm EVs and 300–600-nm EVs. Brackets to the right indicate the 25th, 50th and 75th percentiles of all data; marker and whiskers indicate median and maximum/minimum concentrations of three repeats. [Color figure can be viewed at wileyonlinelibrary.com]

the same model of FCM showed marked differences in performance. For example, of the three BD FACSCanto II FCMs, one could not detect the 400-nm polystyrene beads, one could detect 1200–3000-nm EVs, and one could also detect 600–1200-nm EVs. This discrepancy shows that FCM maintenance, alignment and settings are crucial for optimal results. In fact, another FCM measured a CV of 22% for a 1000-nm polystyrene bead, and probably needed maintenance. Evidence for improper settings can also be found within the data; for example, on one FCM the gain and voltage were set so high that noise on scatter was in the fourth log-decade of a five-log-decade range, resulting in an extremely narrow, and thus useless, detection range. Improper settings are resolvable through training, which is available from several companies and scientific societies in the flow cytometry field. On the positive side, these standardization workshops are a way to benchmark and make improvements. One of the participants who measured and calibrated at several settings to compare performance commented ‘This study has definitely broadened my view of the way in which we analyze EVs on our cytometer and has helped me realize that a few small changes can make a big difference to EV analysis!’.

In this study, we selected a flow rate of 60 $\mu\text{L min}^{-1}$ because this flow rate is available on most FCMs. It is reasonable to assume that a lower flow rate will improve the reproducibility of measurements, provided that the total number of detected platelet-derived EVs is maintained by reducing the sample dilution and/or increasing the measurement time.

See Data S3 for a detailed description of the model approach. Improvements to the model approach may be achievable in three ways: a robust method for determining the scatter resolution limit, refinement of the RI of EVs, and inert beads that mimic EV scatter properties. First, in the present approach, we provided an EV diameter gate when any event was measured at the lower gate boundary.

This procedure is not ideal because, for some FCMs in this study, the background noise on the scatter channel fell within the diameter gate, resulting in an artefactual elevation in EV concentration. The Rosetta Calibration mixture may allow determination of the scatter resolution limit analogous to approaches developed for fluorescence [18]. Second, we assumed that EVs are spheres with a uniform RI of 1.40. Estimates for EV RIs range between 1.37 and 1.45 [10,11,15], and, although the true EV-RI is unknown and may be different for different EV subpopulations, the RI has a profound impact on the calculated diameter of EVs for a particular scatter signal. For example, the same scatter signal is expected for EVs with RIs of 1.37, 1.40 and 1.45 with diameters of 2700, 1200 and 820 nm, respectively. Third, it may be more appropriate to describe EVs as an intravesicular fluid with a low RI that is surrounded by a membrane with a high RI. If the low-RI core-high-RI shell is a good approximation for an EV, a hollow silica bead [Z Varga, M Pálmai, R Garcia-Diez, C Gollwitzer, M Krümrey, JL Fraikin, N Hajji, E van der Pol, TG van Leeuwen, R Nieuwland, under review] may scatter light comparably to EVs of similar diameter. Such a reference bead should have long-term stability as compared with biological reference materials, and may be applied for gating in lieu of the model-based approach. In any case, a scatter-based diameter gate requires the RI of EVs to be approximately constant. If this EV RI is not constant, the alternative approach is to derive the EV diameter by using a fluorescent membrane marker [19], but, thus far, the staining intensity of EVs in plasma samples has been low [20], or has required elaborate protocols [8]. Several of these assumptions are not valid for platelets, which contain dense granules and are discoid. The dense granules are expected to make a substantial contribution to the SSC signal, but less of a contribution to the FSC signal, thus invalidating the assumption that EVs have a uniform RI of 1.40. When comparing volume estimates for

platelets obtained with our model with an impedance-based volume measurement (Fig. S4), we found that the mode platelet volume was underestimated by 30%, and that the mean platelet volume and platelet distribution width were overestimated by two-fold and three-fold, respectively. Because we lack information regarding the shape and contents of large platelet EVs, it is not possible to assess whether an overestimation of diameter occurred in the 1200–3000-nm platelet EV gate.

Taken together, the data presented here suggest that an EV diameter model may be more effective for reducing interlaboratory variability than polystyrene bead-based gating, and that knowledge on the detected EV diameter itself is valuable for the interpretation of results.

Addendum

E. van der Pol, R. Nieuwland, and F. A. W. Coumans were responsible for the conception and design of the study. F. A. W. Coumans was responsible for data collection. E. van der Pol and F. A. W. Coumans were responsible for data analysis and interpretation. E. van der Pol, R. Nieuwland, and F. A. W. Coumans drafted the article. A. Sturk and T. G. van Leeuwen critically revised the article. All authors gave final approval of the version to be published.

Acknowledgements

We acknowledge funding from the ISTH Scientific Standardization Committee on Vascular Biology, and from the Netherlands Organization for Scientific Research – Domain Applied and Engineering Sciences (NWO-TTW), research programs VENI 13681 (F. A. W. Coumans) and Memphis II (E. van der Pol).

Disclosure of Conflict of Interests

E. van der Pol and F. A. W. Coumans are shareholders in Exometry BV. The other authors state that they have no conflict of interest.

Appendix

ISTH-SSC-VB Working Group

F. Mobarrez, Stockholm, Sweden; G. Arkesteijn and M. Wauben, Utrecht, the Netherlands; P. R.-M. Siljander, Helsinki, Finland; V. Sánchez-López and R. Otero-Candelera, Seville, Spain; L. A. Ramón, S. Dolz and V. Vila, Valencia, Spain; N. Mackman and J. Geddings, Chapel Hill, NC, USA; F. Mullier and N. Bailly, Namur, Belgium; J.-Y. Han, Busan, Korea; H. C. Kwaan and I. M. Weiss, Chicago, IL, USA; E. I. Buzás and E. Pállinger, Budapest, Hungary; P. Harrison, Birmingham, UK; J. Kraan, Rotterdam, the Netherlands; B. D. Hedley and A. LazoLangner, London, Ontario, Canada; A. Enjeti,

Newcastle, NSW, Australia; P. J. Norris, San Francisco, CA, USA; C. Paris and S. Susen, Lille, France; A. Bonneyoy and I. Delorme, Montreal, Quebec, Canada; W. L. Chandler, Seattle, Washington, USA; C. Hau, Amsterdam, the Netherlands; H. C. D. Aass, Oslo, Norway; D. Connor, Sydney, NSW, Australia, X. Wu, Seattle, WA, USA; R. Dragovic, Oxford, UK; L. M. Uotila, Helsinki, Finland; R. Lacroix and S. Robert, Marseille, France.

Supporting Information

Additional supporting information may be found online in the Supporting Information section at the end of the article.

Data S1. Further details of samples and distribution.

Data S2. Erythrocyte EV samples.

Data S3. Mie model fitting and extrapolation.

Data S4. Measurement protocol.

Table S1. Diameter of silica beads determined by flow cytometers (FCMs) that measured extracellular vesicles from platelet and erythrocyte samples.

Fig. S1. Estimated size of silica beads compared to bead diameters determined by transmission electron microscopy (TEM).

Fig. S2. The volume distribution of platelets by the scatter model compared to a hematology impedance analyzer.

Fig. S3. Determined concentrations of extracellular vesicles (EVs) from erythrocytes on different flow cytometers for three different gating strategies.

Fig. S4. Determined concentrations of erythrocyte EVs on different flow cytometers for 600–1200-nm EVs and 300–600-nm EVs.

Fig. S5. Size to scatter relationships for FCMs that measured platelet EV and erythrocyte EV samples.

References

- 1 Brisson AR, Tan S, Linares R, Gounou C, Arraud N. Extracellular vesicles from activated platelets: a semiquantitative cryo-electron microscopy and immuno-gold labeling study. *Platelets* 2017; **28**: 1–9.
- 2 Gasecka A, Böing AN, Filipiak KJ, Nieuwland R. Platelet extracellular vesicles as biomarkers for arterial thrombosis. *Platelets* 2017; **28**: 228–34.
- 3 Van Der Pol E, van Gemert M, Sturk A, Nieuwland R, Van Leeuwen T. Single vs. swarm detection of microparticles and exosomes by flow cytometry. *J Thromb Haemost* 2012; **10**: 919–30.
- 4 van der Pol E, Coumans FAW, Gardiner C, Sargent IL, Harrison P, Sturk A, van Leeuwen TG, Nieuwland R. Particle size distribution of exosomes and microvesicles by transmission electron microscopy, flow cytometry, nanoparticle tracking analysis, and resistive pulse sensing. *J Thromb Haemost* 2014; **12**: 1182–92.
- 5 Robert S, Poncelet P, Lacroix R, Arnaud L, Giraudo L, Hauchard A, Sampol J, Dignat-George F. Standardization of platelet-derived microparticle counting using calibrated beads and a Cytomics FC500 routine flow cytometer: a first step towards multicenter studies? *J Thromb Haemost* 2008; **7**: 190–7.
- 6 Lacroix R, Robert S, Poncelet P, Kasthuri R, Key N, Dignat-George F. Standardization of platelet-derived microparticle

- enumeration by flow cytometry with calibrated beads: results of the International Society on Thrombosis and Haemostasis SSC Collaborative workshop. *J Thromb Haemost* 2010; **8**: 2571–4.
- 7 Coite S, Judicone C, Robert S, Mooberry MJ, Poncelet P, Wauben M, Nieuwland R, Key NS, Dignat-George F, Lacroix R. Standardization of microparticle enumeration across different flow cytometry platforms: results of a multicenter collaborative workshop. *J Thromb Haemost* 2016; **15**: 187–93.
 - 8 van der Vlist EJ, Nolte ENM, Stoorvogel W, Arkesteijn GJA, Wauben MHM. Fluorescent labeling of nano-sized vesicles released by cells and subsequent quantitative and qualitative analysis by high-resolution flow cytometry. *Nat Protoc* 2012; **7**: 1311–26.
 - 9 Chandler W, Yeung W, Tait J. A new microparticle size calibration standard for use in measuring smaller microparticles using a new flow cytometer. *J Thromb Haemost* 2011; **9**: 1216–24.
 - 10 Konokhova AI, Yurkin MA, Moskalensky AE, Chernyshev AV, Tsvetovskaya GA, Chikova ED, Maltsev VP. Light-scattering flow cytometry for identification and characterization of blood microparticles. *J Biomed Optics* 2012; **17**: 057006.
 - 11 Gardiner C, Shaw M, Hole P, Smith J, Tannetta D, Redman CW, Sargent IL. Measurement of refractive index by nanoparticle tracking analysis reveals heterogeneity in extracellular vesicles. *J Extracell Vesicles* 2014; **3**: 25361.
 - 12 Maetzler C. *MATLAB functions for Mie scattering and absorption*. Bern: Institute of Applied Physics, University of Bern, 2002.
 - 13 Bohren CF, Huffman DR. *Absorption and Scattering by a Sphere*. *Absorption and Scattering of Light by Small Particles*. New York, NY: Wiley-VCH, 2007: 82–129.
 - 14 van der Pol E, de Rond L, Coumans FAW, Gool EL, Böing AN, Sturk A, Nieuwland R, van Leeuwen TG. Absolute sizing and label-free identification of extracellular vesicles by flow cytometry. *Nanomedicine* 2018; **14**: 801–10.
 - 15 van der Pol E, Coumans FA, Sturk A, Nieuwland R, van Leeuwen TG. Refractive index determination of nanoparticles in suspension using nanoparticle tracking analysis. *Nano Lett* 2014; **14**: 6195–201.
 - 16 Thompson CB, Eaton KA, Princiotta SM, Rushin CA, Valeri CR. Size dependent platelet subpopulations: relationship of platelet volume to ultrastructure, enzymatic activity, and function. *Br J Haematol* 1982; **50**: 509–19.
 - 17 Davis KA, Abrams B, Iyer SB, Hoffman RA, Bishop JE. Determination of CD4 antigen density on cells: role of antibody valency, avidity, clones, and conjugation. *Cytometry* 1998; **33**: 197–205.
 - 18 Chase ES, Hoffman RA. Resolution of dimly fluorescent particles: a practical measure of fluorescence sensitivity. *Cytometry* 1998; **33**: 267–79.
 - 19 Stoner SA, Duggan E, Condello D, Guerrero A, Turk JR, Narayanan PK, Nolan JP. High sensitivity flow cytometry of membrane vesicles. *Cytometry Part A* 2016; **89**: 196–206.
 - 20 de Rond L, van der Pol E, Hau CM, Sturk A, van Leeuwen TG, Nieuwland R, Coumans FAW. Comparison of generic fluorescent dyes for detection of extracellular vesicles by flow cytometry. *Clin Chem* 2018; **64**: 680–689. Under review